Inorganic Chemistry
Cite This: Inorg. Chem. XXXX, XXX, XXX−XXX
Article
pubs.acs.org/IC

Complex Topologies from Simple Building Blocks: Uranium(IV) Thiophosphates

Vladislav V. Klepov and Hans-Conrad zur Loye*

Department of Chemistry and Biochemistry, University of South Carolina, 631 Sumter Street, Columbia, 29208 South Carolina, United States

Supporting Information

ABSTRACT: Six new uranium thiophosphates, $Cs_5Na_6[U(PS_4)_4](PS_4)$ (**1**), $Rb_5Na_3[U(PS_4)_4]$ (**2**), $CsNa[U(PS_4)_2]$ (**3**), $Cs_{1.67}Na_{0.52}I_{0.19}[U(PS_4)_2]$ (**4**), $Cs_{1.033}Na_{1.343}I_{0.376}[U(PS_4)_2]$ (**5**), and $Rb_{1.35}Na_{0.93}I_{0.28}[U(PS_4)_2]$ (**6**), were obtained from halide flux reactions and characterized using single-crystal X-ray diffraction. The structures of these compounds consist of a pseudotetrahedral uranium unit that in combination with a set of PS_4 group coordination modes can result in an isolated $[U(PS_4)_4]^{8-}$ unit, a $[U(PS_4)_2]^{2-}$ chain, or a $[U(PS_4)_2]^{2-}$ slab. Optical and magnetic properties of **3** and **4** were collected. Both compounds exhibit paramagnetic behavior, and $CsNa[U(PS_4)_2]$ (**3**) exhibits a magnetic transition at 200−225 K between two paramagnetic states that both have similar effective magnetic moments of 4.13 and 4.19 μ_B/formula unit, and strong antiferromagnetic interactions with $\theta = -183$ and -172 K, for the high- and low-temperature states, respectively.

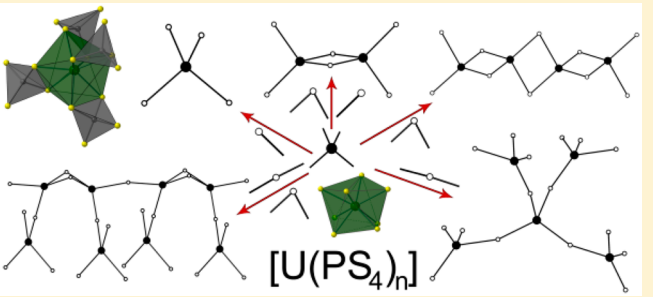

INTRODUCTION

Continuing research focused on preparing new actinide containing compounds is driven by the interest in both the fundamental chemistry and the potential uses of actinide materials. The presence of 5f electrons in the actinide elements has led to their prominent distinction from the rest of the periodic table and gives rise to numerous physical behaviors of their compounds. This difference can be clearly seen from the example of the uranyl cation UO_2^{2+}, which dominates U(VI) chemistry and to a great extent determines structural and physical properties of the uranyl compounds, such as layer topologies and luminescence.[1−7] Although the uranyl cation has always been thought of as a rather strong Lewis acid, it has been shown recently that its strong affinity for sulfur, which is known to be a weak Lewis base, enables the use of layered thiostannates for uranium recovery.[8]

The ongoing research of uranium chemistry is mostly devoted to the synthesis of new U(VI) compounds and the investigation of their physical properties since U(VI) forms readily in an oxygen-rich environment in the presence of oxidizing agents, such as atmospheric oxygen.[9] Most reactions in air therefore result in U(VI) compounds, whereas U(IV) materials are fairly scarce, both due to unintended oxidation of U(IV) to U(VI) during the course of a reaction and due to the undesired formation of the very stable cubic uranium dioxide, UO_2, which exhibits very low reactivity under most synthetic conditions. To overcome this synthetic challenge, other systems based on different anions can be employed. In the chalcogenide series, the closest analogue of oxygen is sulfur. Despite their proximity in the periodic table and their identical outer shell electronic structure, oxygen and sulfur exhibit quite different redox chemistry. In general, since oxygen prefers U(VI), while sulfur prefers U(IV), the majority of the known uranium oxides contain U(VI), while the majority of known sulfides obtained in a sulfur-rich environment contain reduced U(IV).[10,11] The reducing conditions in the sulfide systems and the formation of reduced uranium compounds are highly advantageous for studying 5f electron behavior, i.e., magnetic and optical properties. One downside of sulfides is, however, the sensitivity of these systems to oxygen, where even small amounts present in the reaction mixture can disrupt the formation of the sulfide compounds. Another challenge is to overcome the high moisture sensitivity of the resulting phases, especially those containing thio-anions. The synthesis of the uranium sulfides is, therefore, challenging, but rewarding from the point of view of new topologies that differ significantly from the oxygen-based systems, and thus, potentially, also differ in the exhibited properties.

To date, only a small number of uranium thiophosphate compounds have been reported, some of which exhibit promising structural and magnetic features. Good examples of the structural diversity that uranium thiopshophates offer include the ternary uranium sulfide UP_4S_{12} and the orthothiophosphates $A_{11}U_7(PS_4)_{13}$ (A = K or Rb).[12−14] UP_4S_{12} exhibits a complex 3-fold interpenetrated structure consisting of three UP_4S_{12} diamond-like frameworks where each fills the voids of the others. Magnetic measurements of

Received: June 22, 2018

DOI: 10.1021/acs.inorgchem.8b01733
Inorg. Chem. XXXX, XXX, XXX−XXX

this compound have revealed Curie−Weiss behavior and an effective magnetic moment of 3.84 μ_B along with a large value of θ = −270.6 K, indicating the presence of antiferromagnetic interactions in this compound and magnetic coupling between U atoms through the P_2S_6 ligand.[14] The magnetic susceptibility vs temperature plot shows no transition to a nonmagnetic ground state in U^{4+}, which has been observed in some other U(IV) compounds.[15,16] $A_{11}U_7(PS_4)_{13}$ (A = K or Rb) also exhibit a complex uranium thiophosphate structure, in this case composed of spiral $[U_7(PS_4)_{13}]^{11-}$ chains. $K_{11}[U_7(PS_4)_{13}]$ exhibits an antiferromagnetic transition at about 60 K, and Curie−Weiss behavior at higher temperatures. Its magnetic moment of 2.54 μ_B is significantly lower than the theoretical value of 3.58 μ_B for a $^3H_4$ ground term.[13] It is noteworthy that, along with the isolated PS_4 groups, condensed P_2S_7 and P_3S_{10} units are observed in the uranium thiophosphates UP_2S_7 and $Cs_8U_5(P_3S_{10})(PS_4)_6$, reminiscent of the behavior of the oxyphosphate groups in other uranyl compounds.[12,17−19]

Most reported uranium thiophosphates were synthesized in chalcogenide fluxes containing uranium metal, elemental sulfur, and a phosphorus source, in an evacuated silica tube; in addition, some of them were recrystallized in eutectic halide fluxes. One of the drawbacks of using metallic uranium and elemental sulfur in thiophosphate synthesis is the necessity of low heating rates that afford the initial oxidation of uranium by sulfur.[20,21] This is necessary to allow time for the sulfur to react with the uranium and to avoid sulfur volatilization resulting in high internal pressures that readily burst fused silica tubes. This can be overcome either by not using elemental sulfur or by only using it in very small amounts. A convenient alternative approach is to prereact uranium metal with sulfur to obtain US_2, which can be handled in air. Using US_2 makes it possible to eliminate the very slow heating step, thereby making surveying of the uranium sulfide systems significantly faster. Herein, we report the synthesis and crystal structures of $Cs_5Na_6[U(PS_4)_4](PS_4)$ (**1**), $Rb_5Na_3[U(PS_4)_4]$ (**2**), $CsNa[U(PS_4)_2]$ (**3**), $Cs_{1.67}Na_{0.52}I_{0.19}[U(PS_4)_2]$ (**4**), $Cs_{1.033}Na_{1.343}I_{0.376}[U(PS_4)_2]$ (**5**), and $Rb_{1.35}Na_{0.93}I_{0.28}[U(PS_4)_2]$ (**6**) and magnetic and optical properties of $CsNa[U(PS_4)_2]$ (**3**) and $Cs_{1.67}Na_{0.52}I_{0.19}[U(PS_4)_2]$ (**4**) prepared in halide fluxes containing US_2 as the uranium source.

EXPERIMENTAL SECTION

Caution! *Although the uranium precursor used in this synthesis contains depleted uranium, it is required that proper procedures for handling radioactive materials are observed. All handling of radioactive materials was performed in laboratories specially designated for the study of radioactive actinide materials.*

Reagents. Uranium metal foil (International Bio-Analytical Industries, ACS grade), S powder (Fisher Scientific, sublimed), P_2S_5 (99%, Sigma-Aldrich), Na_2S (Alfa Aesar), CsI (99.9%, Alfa Aesar), RbI (99.8%, Alfa Aesar), and NaI (99.9%, Alfa Aesar) were all used as received.

Uranium sulfide US_2 was obtained by a direct reaction between uranium metal foil and elemental sulfur powder in a stoichiometric ratio. A mixture of 1.00 g of U and 0.2694 g of S (1:2 molar ratio) was loaded in a carbon-coated silica tube in an argon glovebox. The tube with a 10 mm inner diameter was flame-sealed under a pressure of $<10^{-4}$ Torr and placed into a programmable tube furnace at room temperature. The approximate length of the sealed tube is 15 cm. The furnace was ramped up to 650 °C at a rate of 5 °C/h and kept at this temperature for 48 h. The slow heating rate is necessary to avoid pressure buildup inside the tube from sulfur volatilization that will readily burst the fused silica tube by letting the sulfur react completely with the uranium foil. After the reaction was completed, the tube was cooled to room temperature by switching off the furnace. The powder X-ray diffraction pattern of the resulting black powder revealed a small amount of UOS impurity; the source of oxygen in this reaction is most likely an oxide coating on the uranium foil. The amount of the oxysulfide impurity does not exceed 5%, which is acceptable for a flux reaction.

Eutectic fluxes were prepared by taking the respective masses of CsI, RbI, and NaI salts and grinding them together until finely powdered mixture was obtained. The eutectic mixture compositions are 48.5 mol % NaI for CsI−NaI eutectic and 49.4 mol % RbI for CsI−RbI eutectic. The mixtures were placed into open silica tubes and heated to about 50−100 °C above the melting point of the respective eutectic flux (428 °C for CsI−NaI and 579 °C for CsI−RbI eutectic) and kept at this temperature for several hours. After cooling back down to room temperature, the eutectic mixtures were removed from the tube, ground, and immediately used.

Synthesis. In all cases, the starting reagents, US_2, Na_2S, P_2S_5, and the respective flux, were mixed inside a silica tube located inside a nitrogen glovebag. The reagent filled silica tubes were flame-sealed under a vacuum of $<10^{-4}$ Torr and placed vertically into a programmable box furnace. The furnace was heated to the target temperature in 1.5 h and held at this temperature for 6−20 h depending on the specific reaction, see details below. Following this heating step, the furnace was cooled to below the melting point of the flux at a rate between 6 and 10 °C/h to effect the formation of crystallized products. Once at room temperature, the tube was cut open and the end of the tube containing the reaction products was placed into a beaker filled with a dry alcohol, either methanol or ethanol. After sonicating for between 1 and 3 h, the reaction mixture could be extracted from the tube. The solution above the reaction products was decanted and replaced with a fresh portion of solvent at which point sonication was repeated. This procedure was performed several times until most or all of the flux was removed from the product, which was then stored under the solvent to prevent its direct contact with air. All the products were found to be moisture-sensitive.

*$Cs_5Na_6[U(PS_4)_4](PS_4)$ (**1**).* This compound was obtained by a reaction between US_2, Na_2S, and P_2S_5 in a molar ratio of 1:2:1 using 0.10 g of US_2 and 1.50 g of CsI as a flux. The reaction was carried out at a temperature of 750 °C in the course of 20 h, and then cooled to 550 °C in 20 h (cooling rate 10 °C/h). After sonication in methanol and filtration, the product was found to be a mixture of undissolved flux and unidentified phases along with small yellow blocks of **1**. The approximate yield of **1** did not exceed 10%.

*$Rb_5Na_3[U(PS_4)_4]$ (**2**).* This compound was obtained following a similar synthetic procedure used for **1** except that the CsI flux was replaced with RbI. The same molar ratio of 1:2:1 and uranium sulfide sample mass were used along with 1.00 g of RbI flux. After heating, the reaction was kept at 720 °C for 12 h and then cooled to 520 °C at a rate of 10 °C/h. Similar to **1**, yellow blocks of **2** were obtained in a relatively low yield not exceeding 10% after sonication with methanol and filtration.

*$CsNa[U(PS_4)_2]$ (**3**).* This compound was obtained in 1.00 g of NaI and CsI eutectic flux by using a 1:2:2 molar ratio of US_2 (0.10 g), Na_2S, and P_2S_5. The reaction was dwelled at 500 °C for 20 h and cooled to 350 °C in 25 h, cooling rate 6 °C/h. The product was sonicated with anhydrous ethanol until black block crystals with a small amount of undissolved flux were obtained. This mixture was treated with distilled water for several minutes to dissolve the remaining flux and then filtered and washed with ethanol. The resulting black phase was found to be phase pure and used for studying magnetic and optical properties. The yield of the reaction is about 60%.

*$Cs_{1.67}Na_{0.52}I_{0.19}[U(PS_4)_2]$ (**4**).* This compound was obtained from 1.00 g of NaI and CsI eutectic flux using a 1:2:2 molar ratio of US_2, Na_2S, and P_2S_5 with a larger (as compared to the previous three reactions) starting amount of US_2 (0.20 g) and proportionally the other reagents. Similar to **3**, the reaction was kept at 500 °C for 48 h and then cooled to 350 °C in 25 h with a cooling rate of 6 °C/h. The product was purified by sonicating the mixture for about 6 h, changing the solvent, anhydrous ethanol, by decantation every half an hour.

DOI: 10.1021/acs.inorgchem.8b01733
Inorg. Chem. XXXX, XXX, XXX−XXX

Table 1. Crystallographic Data for 1−6

	1	2	3	4	5	6
chemical formula	$Cs_5Na_6[U(PS_4)_4](PS_4)$	$Rb_5Na_3[U(PS_4)_4]$	$CsNa[U(PS_4)_2]$	$Cs_{1.67}Na_{0.52}I_{0.19}[U(PS_4)_2]$	$Cs_{1.033}Na_{1.343}I_{0.376}[U(PS_4)_2]$	$Rb_{1.35}Na_{0.93}I_{0.28}[U(PS_4)_2]$
fw	1836.57	1371.19	712.35	814.48	772.38	728.75
cryst syst	orthorhombic	orthorhombic	monoclinic	orthorhombic	orthorhombic	orthorhombic
space group, Z	*Ama*2, 4	$P2_12_12$, 2	*C*2/*c*, 4	*Aba*2, 20	*Fdd*2, 40	*Ccc*2, 20
a, Å	16.7652(7)	18.0244(5)	9.7350(2)	37.2808(9)	72.7960(14)	10.6283(5)
b, Å	24.3661(8)	8.6694(3)	18.4642(4)	11.0386(3)	11.0715(2)	20.1263(10)
c, Å	9.8909(3)	10.1249(3)	8.7452(2)	19.6835(6)	19.4286(4)	37.1835(17)
β, deg	90	90	123.4570(10)	90	90	90
V, Å^3	4040.5(2)	1582.12(8)	1311.47(5)	8100.3(4)	15658.7(5)	7953.9(7)
ρ_{calcd}, g/cm^3	3.019	2.878	3.608	3.339	3.276	3.043
radiation (λ, Å)	Mo Kα (0.710 73)	Mo Kα (0.710 73)	Mo Kα (0.710 73)	Mo Kα (0.710 73)	Mo Kα (0.710 73)	Mo Kα (0.710 73)
μ, mm^{-1}	9.760	14.070	16.614	15.284	14.744	16.089
T, K	300(2)	300(2)	300(2)	300(2)	300(2)	300(2)
crystal dimensions, mm^3	0.07 × 0.05 × 0.04	0.06 × 0.04 × 0.04	0.05 × 0.04 × 0.01	0.04 × 0.02 × 0.01	0.12 × 0.04 × 0.01	0.12 × 0.06 × 0.03
2θ range, deg	2.533−28.280	3.026−27.499	2.740−32.491	2.185−28.295	2.136−27.495	2.167−27.498
no. of reflns collected	12 290	25 021	46 359	37 153	44 275	54 167
no. of data/restraints/params	4913/1/180	3624/0/138	2372/0/61	9268/1/332	7961/1/348	7927/19/388
R_{int}	0.0431	0.0301	0.0277	0.0672	0.0323	0.0431
GOF	1.049	1.166	1.121	1.097	1.047	1.120
R_1 ($I > 2\sigma(I)$)	0.0393	0.0471	0.0088	0.0615	0.0361	0.0502
wR_2 (all data)	0.0829	0.1244	0.0213	0.1255	0.1011	0.1314

The resulting product was found to be dark red/black plate-like crystals with no visible signs of impurities or undissolved flux in it. Due to rapid decomposition of crystals of **4** upon contact with water or air moisture, all measurements were performed without grinding them. The yield of the reaction is approximately 40%.

*$Cs_{1.033}Na_{1.343}I_{0.376}[U(PS_4)_2]$ (**5**).* This compound was obtained by reacting US_2 (0.10 g) with Na_2S and P_2S_5 in a 1:4:4 molar ration in 1.00 g of CsI and NaI eutectic flux. The reaction was carried out at 600 °C in 20 h and cooled to 360 °C in 24 h. The product was sonicated in dry ethanol and then filtered and washed with an abundant amount of ethanol. Despite multiple sonication cycles and decanting unreacted flux, the resulting product was found to be a mixture of dark red plate crystals with unidentified impurities. The yield of the red crystals is about 40%.

*$Rb_{1.35}Na_{0.93}I_{0.28}[U(PS_4)_2]$ (**6**).* This compound was obtained along with the previously reported $Rb_{11}U_7(PS_4)_{13}$. A mixture of US_2 (0.05 g), Na_2S, P_2S_5, and 1.50 g of RbI flux was heated in an evacuated silica tube up to 720 °C and kept at this temperature for 20 h. After this, the reaction was slowly cooled to 540 °C at a rate of 10 °C/h. The product was sonicated in dry ethanol and filtered. Examination of the mixture revealed the presence of at least two phases, black block crystals of $Rb_{11}U_7(PS_4)_{13}$,[13] and red plate crystals of **6**. At this reaction condition the yield of **6** was quite small, less than 10%, and no attempts were made to improve it since single-crystal X-ray diffraction data revealed a close resemblance between **6** and **4**, which was obtained as a phase pure sample.

Single-Crystal X-ray Diffraction. Single-crystal X-ray diffraction data were collected at 300(2) K on a Bruker D8 QUEST diffractometer equipped with an Incoatec IμS 3.0 microfocus radiation source (Mo Kα, λ = 0.71073 Å) and a PHOTON II area detector. The crystals were mounted on a microloop with immersion oil. The raw data reduction and absorption correction were performed using SAINT and SADABS programs.[22,23] Initial structure solutions were obtained with SHELXS-2017 using direct methods and Olex2 GUI.[24] Full-matrix least-squares refinements against F^2 were performed with SHELXL software.[25] All the structures were checked for missing symmetry with the Addsym program implemented into PLATON software, and no higher symmetry was found.[26] The crystallographic data and results of the diffraction experiments are summarized in Table 1.

The structure models of **4**−**6** reported herein show reliably only the arrangement of U, P, and S atoms, whereas disordered Cs, Na, Rb, and I positions are assigned to match the electron density present within and between the slabs, conserving the charge balance. The presence of these elements and their approximate ratio were positively confirmed by EDS.

Powder X-ray Diffraction. Powder X-ray diffraction (PXRD) data for phase purity confirmation were collected on polycrystalline samples ground from single crystals for **3** or crystalline sample of **4** (Figure S1 and S2). Data for **3** and **4** were collected on a Bruker D2 PHASER and a Rigaku Ultima IV diffractometer, respectively, using Cu Kα radiation. The data were collected over 2θ ranges 10−65° with a step size of 0.02°.

Energy-Dispersive Spectroscopy (EDS). EDS was performed on product single crystals using a Tescan Vega-3 SEM equipped with a Thermo EDS attachment. The SEM was operated in low-vacuum mode. Crystals were mounted on an SEM stub with carbon tape and analyzed using a 20 kV accelerating voltage and an 80 s accumulation time. The results of EDS confirm the presence of elements found by single-crystal X-ray diffraction (Figure S3 and Table S1).

Optical Properties. UV−vis spectra for **3** and **4** were recorded using a PerkinElmer Lambda 35 UV−vis scanning spectrophotometer used in the diffuse reflectance mode and equipped with an integrating sphere (Figure S4). Diffuse reflectance spectra were recorded in the 200−900 nm range. Reflectance data were converted to absorbance using the Kubelka−Munk function.

Magnetism. Magnetic property measurements were performed using a Quantum Design MPMS 3 SQUID magnetometer. Zero-field-cooled (ZFC) magnetic susceptibility measurements were performed from 2 to 300 K for **4** or 375 K for **3** in an applied field of 0.1 T. The raw data were corrected for radial offset and sample shape effects according to the method described in the literature.[27]

Topological Analysis and Crystal Chemical Calculations. Crystal structure analysis was performed using the TOPOS 4.0 software package.[28,29] The method of intersecting spheres was employed for coordination number determination using the AutoCN program.[30] Dirichlet and ADS programs were employed for Voronoi−

DOI: 10.1021/acs.inorgchem.8b01733
Inorg. Chem. XXXX, XXX, XXX−XXX

Dirichlet polyhedra construction and topological analysis, respectively. The standard structure simplification procedure was employed to obtain the underlying nets of the compounds.[31]

RESULTS AND DISCUSSION

Synthesis. In this work, the US_2−Na_2S−P_2S_5 system was explored by synthesizing new compositions employing fast reagent heating rates followed by multihour dwells at temperatures ranging from 500 to 750 °C. Initial synthesis attempts using alkali chloride fluxes did not result in the desired thiophosphate phases. Specifically, several reactions using US_2:Na_2S:P_2S_5 in ratios varying from 1:1:1 to 1:4:4 in a CsCl flux at temperatures in excess of 750 °C were unsuccessful, yielding primarily black uranium sulfide and/or sodium uranium sulfide powders. Consequently, the reaction conditions were modified by substituting lower melting point alkali iodide fluxes for the alkali chloride fluxes, since one might expect that the larger iodide anion would be more favorable for dissolving and providing a reaction environment more suitable for the rather large sulfide and thiophosphate anions. When the reaction temperatures were decreased to 750 °C, the first thiophosphate, $Cs_5Na_6[U(PS_4)_4](PS_4)$ (**1**), was successfully obtained by this route. Further investigation using a RbI flux resulted in the synthesis of $Rb_5Na_3[U(PS_4)_4]$ (**2**) and $Rb_{1.35}Na_{0.93}I_{0.28}[U(PS_4)_2]$ (**6**). Obtaining other new thiophosphate phases at lower reaction temperatures was the main reason for using the iodide eutectic fluxes CsI−NaI and RbI−NaI, which allowed us to decrease the operating temperature range of the fluxes to 500−600 °C, resulting in the synthesis of the other three compounds $CsNa[U(PS_4)_2]$ (**3**), $Cs_{1.67}Na_{0.52}I_{0.19}[U(PS_4)_2]$ (**4**), and $Cs_{1.033}Na_{1.343}I_{0.376}[U(PS_4)_2]$ (**5**).

Some compositional modifications of compounds **4**−**6** with varying ratios of the alkali halide in the structure can also be obtained utilizing slightly modified reaction conditions; however, all of them are based on the same $[U(PS_4)_2]^{2-}$ slabs and crystallize in one of the three space groups *Ccc*2 (No. 37), *Aba*2 (No. 41), and *Fdd*2 (No. 43) observed for compounds **4**−**6**. These compositional variants are almost identical and are therefore are not reported herein.

Apart from temperature, an important impact of the flux quantity used in the synthesis for affecting phase formation was observed. As a good example of this impact, we can contrast the syntheses of **3** and **4**. In both cases, the molar ratio of US_2:Na_2S:P_2S_5 in the initial mixture and the reaction temperature were the same, and only the relative amount of flux was changed. In a more "diluted" reaction, when 1.00 g of CsI and NaI eutectic is used to dissolve 0.10 g of US_2 and the respective amounts of the other reagents, the resulting product is a phase pure sample of **3** with a decent yield of about 60%, whereas a doubled amount of the starting reagents (0.20 g of US_2) produces crystals of **4**.

Choosing a solvent to dissolve and remove the flux and isolate reaction products is quite challenging in this system. First, the solvent should be polar for dissolving the ionic cesium and rubidium halide fluxes, and second, it should not contain water, which quickly degrades the reaction products; all compositions, with the exception of **3**, are extremely sensitive to water. This limits the solvent choice to commonly available dry solvents: acetone, acetonitrile, DMSO, DMF, and alcohols. Initial trials showed that neither acetonitrile nor acetone are very efficient in halide flux dissolution, whereas both DMF and DMSO tend to dissolve the products of the reactions, resulting in a red solution. Therefore, the remaining choice fell on dry alcohols, such as methanol and ethanol, which demonstrate a fair ability to dissolve fluxes, as compared to the other solvents, and usually do not dissolve the products. However, one should be careful about using dry alcohol as a solvent in the presence of unreacted P_2S_5, because a reaction between them quickly results in the undesired contamination of the reaction product by yellow crystals of $Cs_2[S_3POCH_3]$, $Cs[S_2P(OCH_3)_2]$, and $Cs_2[S_3POC_2H_5]$, whose crystal structures will be reported elsewhere. These reactions are related to the process for obtaining zinc dialkyldithiophosphates, which are used as lubricants and antiwear additives, and which form upon treating P_2S_5 with ethanol and ZnO.[32] However, the formation of methoxy- and ethoxythiophosphates can easily be avoided by regularly, every 30 min, decanting the solution above the product and replacing it with a fresh portion of a solvent.

Structure Description. In the structures of **1**−**6**, the uranium atoms are surrounded by S atoms with U−S bond lengths of 2.745(7)−2.983(9) Å with an average interatomic distance of 2.84(5) Å, agreeing well with the bond distances in previously reported uranium thiophosphates.[12,33] The Voronoi polyhedron volume of the uranium atoms falls within a narrow range 19.0−19.4 $Å^3$ with an average of 19.2(1) $Å^3$, indicating the same oxidation state for the uranium atoms in all six structures. The charge assignment in **1**−**3** is rather straightforward, and the uranium atoms in these three structures are all in the +4 oxidation state. In all six structures, the uranium atoms are 8-fold coordinated and form a coordination polyhedron in the shape of a trigonal dodecahedron.[34] The phosphorus atoms in these three structures form thiophosphate groups PS_4^{3-}. The P−S bond lengths and S−P−S angles fall within the ranges 1.969(11)−2.086(5) Å (average 2.04(3) Å) and 96.4(7)−118.0(9)°, in good agreement with previously reported values.[10,12]

$Cs_5Na_6[U(PS_4)_4](PS_4)$ (**1**) and $Rb_5Na_3[U(PS_4)_4]$ (**2**) crystallize in the orthorhombic space groups *Ama*2 and $P2_12_12$, respectively. Compound **1** consists of two main anionic structural units, $[U(PS_4)_4]^{8-}$ and PS_4^{3-} (Figure 1),

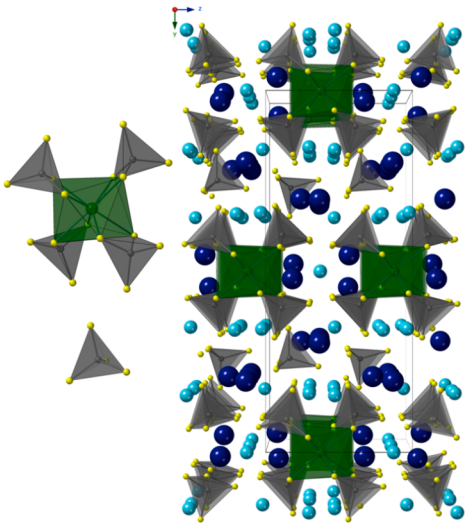

Figure 1. Main structural units (top left) $[U(PS_4)_4]^{8-}$ and (bottom left) PS_4^{3-} and (right) a view down the *a* axis of $Cs_5Na_6[U(PS_4)_4](PS_4)$ (**1**). US_8 and PS_4 polyhedra are green and gray; sodium and cesium atoms are shown in cyan and dark blue, respectively.

DOI: 10.1021/acs.inorgchem.8b01733
Inorg. Chem. XXXX, XXX, XXX−XXX

connected to each other via intervening alkali cations; in contrast, **2** only contains the $[U(PS_4)_4]^{8-}$ structural unit (Figure 2). Both structures contain a single-crystallographic uranium site, U1, which is located on a position with C_2 site-symmetry. Each of the four tetrahedral thiophosphate groups forming the $[U(PS_4)_4]^{8-}$ complex are edge-sharing with the uranium polyhedron, adopting a B^{01} coordination type (the letter B refers to a bidentate coordination mode of the thiophosphate group, and the superscript numbers show the number of corner- and edge-shares, respectively).[35] The fifth thiophosphate group in **1** is isolated from the uranium complex and binds only to the alkali cations. The cesium, rubidium, and sodium atoms are surrounded by the sulfur atoms of the thiophosphate groups with Cs−S, Rb−S, and Na−S bond lengths of 3.403(4)−3.888(4), 3.264(6)−3.732(5), and 2.816(8)−3.202(9) Å, respectively.

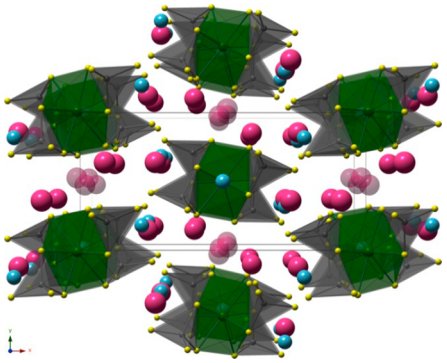

Figure 2. View of the structure of $Rb_5Na_3[U(PS_4)_4]$ (**2**) down the *c* axis. US_8 and PS_4 polyhedra are green and gray; sodium and rubidium atoms are shown in cyan and pink, respectively. Disordered Rb sites are translucent.

$CsNa[U(PS_4)_2]$ (**3**) crystallizes in the *C*2/*c* space group and is based on $[U(PS_4)_2]^{2-}$ chains, consisting of edge-sharing US_8 polyhedra, extending along the *c* axis (Figure 3). Each uranium atom is connected to four thiophosphate groups by edge-sharing, whereas each thiophosphate group bridges two uranium atoms and plays the role of a tridentate ligand sharing two adjacent edges with two different metal sites, corresponding to T^{02} coordination type. The chains are connected to each other through intervening alkali cations. The Cs−S and Na−S bonds are 3.5895(4)−3.8497(4) and 2.8082(5)−3.3087(10) Å, respectively, which all fall within the expected ranges.

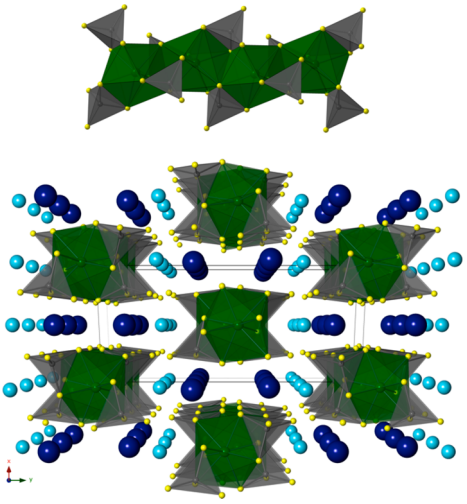

Figure 3. (Top) Single $[U(PS_4)_2]^{2-}$ chain and (bottom) the structure of $CsNa[U(PS_4)_2]$ (**3**) viewed down the *c* axis. US_8 and PS_4 polyhedra are green and gray; sodium and cesium atoms are shown in cyan and dark blue, respectively.

$Cs_{1.67}Na_{0.52}I_{0.19}[U(PS_4)_2]$ (**4**), $Cs_{1.033}Na_{1.343}I_{0.376}[U(PS_4)_2]$ (**5**), and $Rb_{1.35}Na_{0.93}I_{0.28}[U(PS_4)_2]$ (**6**) are all based on the same complex slabs and differ by the composition and arrangement of the severely disordered alkali halides residing both in the pores within the slabs and in between the slabs (Figure 4a). The top and bottom part of each slab consists of parallel chains (Figure 4c,d), rotated by about 60° relative to each other. Each $U(PS_4)_4$ group between them connects two chains from above and two from below it, resulting in an infinite sandwich structure. The slab cation topology is a 2-periodic net consisting of 3- and 4-coordinated nodes. Due to the arrangement of the chains at different levels, the slab topology cannot be depicted in two dimensions without edge crossing and is therefore a 3-dimensional net.

In **4**−**6**, there are three crystallographically unique uranium atoms. Both U1 and U2 sites form the chains, and the third site, U3, links the chains into a single slab. The U1 and U2 sites are coordinated by four thiophosphate groups in a bidentate mode and share edges with each other. Two of the four thiophosphate groups share two adjacent edges with uranium atoms, whereas the other two share their opposite two edges, corresponding to tridentate T^{02} and tetradentate Q^{02} coordination types, respectively (Figure 5). At the same time, all four thiophosphate anions coordinated by the third uranium site U3 are of the Q^{02} coordination type.

Structural Features of Uranium Orthothiophosphates. To date, only seven uranium orthothiophosphates have been reported in the literature.[12,13,17,36,37] Together with the compounds reported herein, their number almost doubles, enabling an, albeit limited, crystallographic analysis. In all cases, except for one crystallographic type of uranium atoms in $M_{11}U_7(PS_4)_{13}$ (M = K, Rb), the coordination number of uranium atoms is 8, and each uranium atom is surrounded by four thiophosphate groups so that the phosphorus atoms are arranged in a distorted tetrahedral mode around the central uranium atom.[12] There are three common coordination types for the thiophosphate anions, B^{01}, T^{02}, and Q^{02} (Figure 5). The B^{01} thiophosphate unit functions as a terminal building block that shares an edge with the uranium polyhedron. The T^{02} and Q^{02} thiophosphate units both share two edges with the uranium polyhedra, where T^{02} uses its three sulfur atoms to bind the uranium atoms, and therefore serves as a triangular linking unit (Figure 5c), while the tetrahedral Q^{02} thiophosphate group shares its two opposing edges with the uranium atoms (Figure 5d), playing the role of a linear linker. The T^{02} groups can form two types of dimeric units, planar and bent (Figure 5e,f). Combined with the tetrahedral arrangement around the uranium centers, the uranium metal nodes can be connected by the thiophosphate linkers in only a limited number of possible topologies, some of which are realized in the reported compounds (Figure 6).

As shown in Figure 6a, a combination of the uranium metal node with four terminal B^{01} units results in an isolated $[U(PS_4)_4]^{8-}$ complex, which is observed for the first time in $Cs_5Na_6U(PS_4)_5$ and $Rb_5Na_3U(PS_4)_5$. It is noteworthy that the "abundant" fifth thiophosphate group in $Cs_5Na_6U(PS_4)_5$ does

DOI: 10.1021/acs.inorgchem.8b01733
Inorg. Chem. XXXX, XXX, XXX−XXX

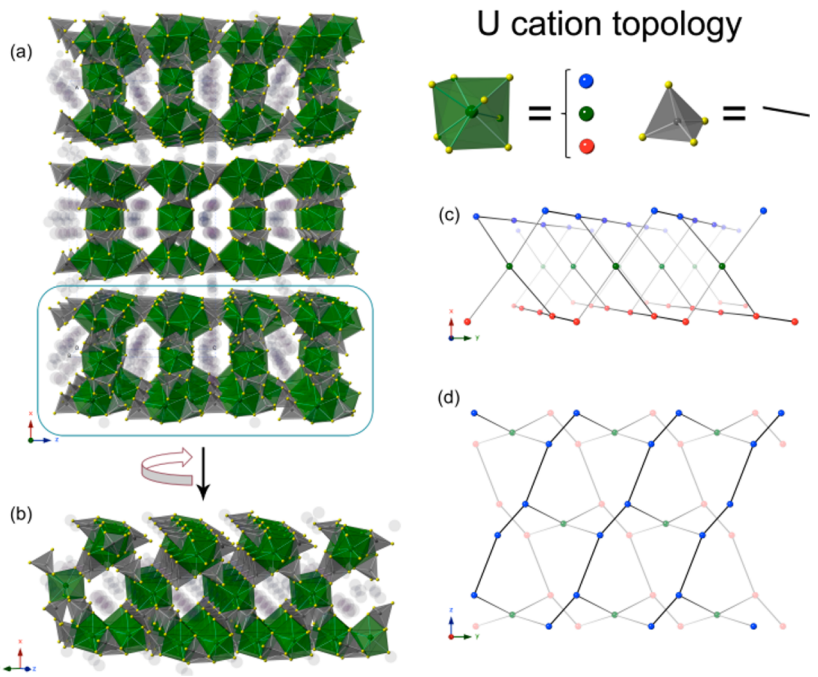

Figure 4. (a) View of the crystal structure of $Cs_{1.67}Na_{0.52}I_{0.19}[U(PS_4)_2]$ (**4**) and (b) its main structural unit, the $[U(PS_4)_2]^{2-}$ slab, that consists of chains connected through uranium metal nodes seen in parts c and d which illustrate the cation topology of the slabs. The uranium metal nodes at different levels are shown in different colors. US_8 and PS_4 polyhedra are green and gray. Disordered sodium, cesium, and iodine atoms are faded for clarity.

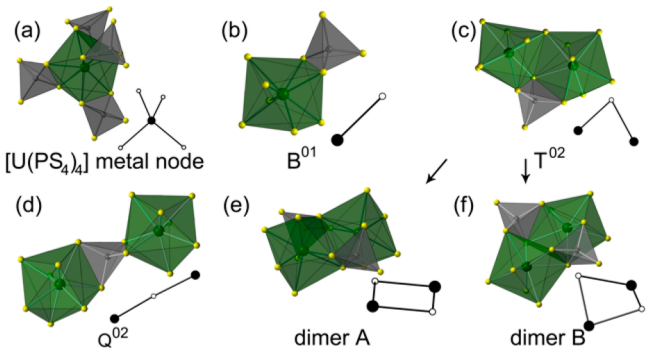

Figure 5. (a) Uranium coordination environment and (b–d) coordination types of the thiophosphate anions in **1**–**6**. Parts e and f show possible aggregation of two uranium atoms by two T^{02} thiophosphate units in a planar (e) or a bent (f) dimer.

not participate in the bonding with the uranium center, suggesting that the uranium center, tetrahedrally surrounded by four edge-sharing thiophosphate groups, is a structurally stable complex, which justifies the designation of the metal tetrahedral node as a main building unit. Another isolated complex can be obtained from two uranium centers connected by two T^{02} groups in a planar mode (dimer A in Figure 5e). The remaining four edges are shared by terminal B^{01} groups (Figure 6b), resulting in the $[U_2(PS_4)_6]^{10-}$ dimer observed in $K_5U(PS_4)_3$.[17] There is a possible combination of one linear Q^{02} thiophosphate linker with six of the B^{01} terminal groups, which would result in a dimer with a $[U_2(PS_4)_7]^{13-}$ composition; however, such dimers have not been observed so far.

Polymeric structural units can form in the absence of the terminal B^{01} linkers. The chains observed in $CsNa[U(PS_4)_2]$, $Sr[U(PS_4)_2]$, and $Ba[U(PS_4)_2]$ can all be represented as a combination of n uranium metal nodes and $2n$ T^{01} bridging units successively arranged in a planar fashion (Figure 6c).[36] Another possible combination with the same stoichiometry, but replacing T^{01} units with Q^{02} groups, can result only in a 3D structural motif, because the Q^{02} thiophosphate groups are linear and the metal centers are tetrahedrally surrounded by them. The underlying net of the resulting structure can be any of the nets with 4-coordinated nodes, such as diamond **dia** or lonsdaleite **lon**.[38,39] The only compound observed of this type is $CsLiU(PS_4)_2$ with the **nbo** topology.[39] It is noteworthy that an ideal **nbo** net is based on planar square nodes, whereas the metal nodes in $CsLiU(PS_4)_2$ have pseudotetrahedral coordination, meaning that a distorted tetrahedral coordination would favor, but not necessarily result, in a tetrahedral net. One can therefore envision compounds exhibiting other topologies based on 4-coordinated nodes, not restricted exclusively to nets with tetrahedral nodes. The most complex topology in this series observed so far, which is built using a combination of three crystallographic types of the metal nodes and both T^{02} and Q^{02} groups, is the slab found in **4**–**6**. Two crystallographic uranium nodes form chains, in which the nodes are successively connected by either one Q^{02} group or two T^{02} groups in the bent dimer B mode (Figure 5f). The fourth vacancy of both metal nodes in the chains is occupied by a Q^{02} group, which bridges them to the third unique metal node (Figure 6e). These structures are a good illustration of how complicated a combination of a distorted tetrahedral metal node with three different linker units, one of them a terminal one, can be. Due to this, one can expect that in the future additional complex topologies will be discovered in the uranium thiophosphate system.

UV–Vis Diffuse Reflectance Spectra. In the reported compounds the uranium metal centers are surrounded by sulfur atoms, which changes the optical properties significantly from that of typical oxide and fluoride compounds.[15,40–42] Instead of several prominent absorption maxima in a range

DOI: 10.1021/acs.inorgchem.8b01733
Inorg. Chem. XXXX, XXX, XXX–XXX

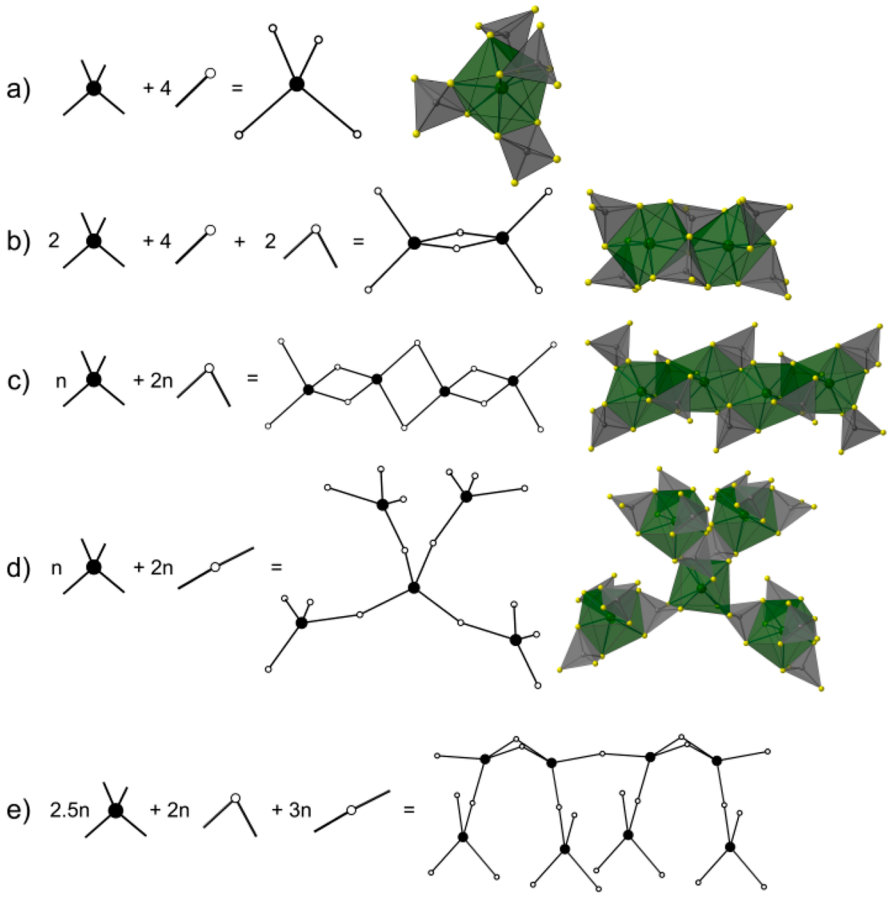

Figure 6. Combination of the uranium metal nodes with thiophosphate linkers resulting in the topologies observed in the uranium orthothiophosphates. (a) Combination of the metal node with B^{01} units resulting in an isolated $[U(PS_4)_4]^{8-}$ complex ($Cs_5Na_6U(PS_4)_5$ and $Rb_5Na_3U(PS_4)_4$ reported herein). (b) A dimer built of two T^{02} and four terminal B^{01} units ($K_5U(PS_4)_3$[17]). (c) Illustration of the formation of infinite chains by a combination of *n* metal nodes and 2*n* T^{02} units ($CsNaU(PS_4)_2$, $SrU(PS_4)_2$, and $BaU(PS_4)_2$).[36] (d) The combination of linear Q^{02} units and the uranium metal nodes results in a framework observed in $CsLiU(PS_4)_2$.[39] (e) Illustration of the combination of 2.5*n* metal nodes, 2*n* occupying general positions and one special position, with 2*n* T^{02} and 3*n* Q^{02} thiophosphate groups to build a fragment of the slab observed in **4**–**6** (shown in Figure 4).

400–700 nm observed for uranium(IV) atoms in oxygen environments,[40] the UV–vis spectra of **3** and **4** (Figure S2) exhibit a sharp absorption band at ∼750 nm and a broad absorption band in the range 400–625 nm, which is consistent with the color of their crystals. The absorption bands at ∼750 nm have been associated with ligand-to-metal charge-transfer.[17]

Magnetic Properties. The magnetic susceptibility χ versus temperature T data for compounds **3** and **4** were collected in an applied field of 0.1 T. The $\chi(T)$ and $1/\chi(T)$ plots for **3** and **4** are shown in Figure 7 and Figure S5. Compound **4** exhibits simple paramagnetic behavior from approximately 50 to 300 K. The effective moment μ_{eff} calculated by fitting the inverse susceptibility vs T plot was found to be 3.09 μ_B, and the Weiss constant for this compound is −66.3 K, indicating antiferromagnetic interactions between the uranium atoms. It is important to note that the magnetic measurements on **4** were performed using a sample that was not ground into a powder. Considering the plate-like morphology of the crystal, it is possible that the measurement is affected by possible preferred orientation effects, which could impact the effective magnetic moment. Compound **3** displays a more complex magnetic behavior, which consists of two paramagnetic regimes with a transition between them. The high-temperature paramagnetic

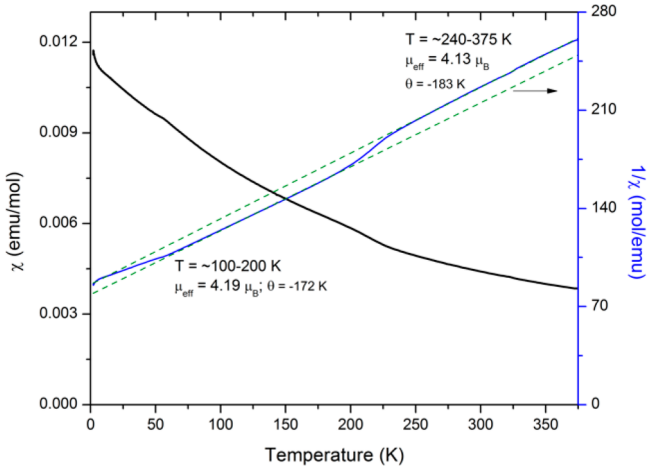

Figure 7. Temperature dependence of the molar and inverse molar susceptibilities of $CsNaU(PS_4)_2$ (**3**).

phase exists in the temperature range 240–375 K, follows Curie–Weiss behavior, and yields an effective moment μ_{eff} of 4.13 μ_B and θ = −183 K. The $1/\chi(T)$ plot clearly exhibits a phase transition in the 200–225 K temperature range. The low-temperature region, which also follows the Curie–Weiss

DOI: 10.1021/acs.inorgchem.8b01733
Inorg. Chem. XXXX, XXX, XXX–XXX

law, has a slightly different effective moment (4.19 μ_B) and Weiss constant (−172 K). There is a distinguishable third transition in a temperature range below 100 K, which suggests a return to the high-temperature mode; however, there are not enough data points at low temperatures to establish this unambiguously. Large absolute values of Weiss constant for both low- and high-temperature states can serve as an indication of antiferromagnetic interactions in the $[U(PS_4)_2]^{2-}$ chains present in this compound. In order to reveal the nature of the transition at 200−225 K, which could be triggered by a structural change, single-crystal X-ray diffraction data at 100 K were collected from a crystal of $CsNaU(PS_4)_2$. The structure refinement using the high-temperature model with the low-temperature data set revealed no significant change in the structure, besides the expected slight bond length contractions. Therefore, the transition is likely due to a change in the electronic structure of the uranium atoms; however, at this time, no definitive conclusion can be drawn in the absence of additional information on this system.

CONCLUSION

A series of new uranium(IV) thiophosphates $Cs_5Na_6[U(PS_4)_4](PS_4)$ (**1**), $Rb_5Na_3[U(PS_4)_4]$ (**2**), $CsNa[U(PS_4)_2]$ (**3**), $Cs_{1.67}Na_{0.52}I_{0.19}[U(PS_4)_2]$ (**4**), $Cs_{1.033}Na_{1.343}I_{0.376}[U(PS_4)_2]$ (**5**), and $Rb_{1.35}Na_{0.93}I_{0.28}[U(PS_4)_2]$ (**6**) was prepared via a high-temperature flux crystal growth method in evacuated silica tubes. Compounds **1**−**6** are based on pseudotetrahedral uranium metal nodes and thiophosphate anions adopting terminal B^{01}, and bridging T^{02} and Q^{02} coordination modes. Their combination gives rise to different topologies, some of which have been observed in the reported uranium compounds, e.g., an isolated $[U(PS_4)_4]^{8-}$ complex in **1** and **2**, a dimer in $K_5U(PS_4)_3$, a chain in **3**, and a complex slab in **4**−**6**. Linking the uranium nodes with linear Q^{02} thiophosphate units results in the **nbo** framework topology of $CsLiU(PS_4)_2$. Several additional topologies can arise from such a combination, i.e., diamond **dia** and lonsdaleite **lon**, that has not been observed so far, but that can possibly be obtained in the presence of properly selected counter cations.

Optical spectra of **3** and **4** are consistent with the previously reported data for other uranium thiophosphates. Magnetic measurements revealed the presence of antiferromagnetic interactions in both compounds and effective moments that are in good agreement with previously reported data. Compound **3** exhibits a magnetic transition in the 200−225 K temperature range, transitioning from one paramagnetic state to another, in the absence of any significant structural change. A likely cause for this is a change in the electronic structure of the uranium as a function of temperature.

ASSOCIATED CONTENT

Supporting Information

The Supporting Information is available free of charge on the ACS Publications website at DOI: 10.1021/acs.inorgchem.8b01733.

PXRD patterns for **3** and **4**, SEM images of **1**−**6**, UV−vis spectra for **3** and **4**, and magnetic susceptibility versus temperature plot for **4** (PDF)

Accession Codes

CCDC 1850953−1850958 contain the supplementary crystallographic data for this paper. These data can be obtained free of charge via www.ccdc.cam.ac.uk/data_request/cif, or by emailing data_request@ccdc.cam.ac.uk, or by contacting The Cambridge Crystallographic Data Centre, 12 Union Road, Cambridge CB2 1EZ, UK; fax: +44 1223 336033.

AUTHOR INFORMATION

Corresponding Author

*E-mail: zurloye@mailbox.sc.edu.

ORCID

Hans-Conrad zur Loye: 0000-0001-7351-9098

Notes

The authors declare no competing financial interest.

ACKNOWLEDGMENTS

Research was supported by the US Department of Energy, Office of Basic Energy Sciences, Division of Materials Sciences and Engineering, under award DE-SC0008664 and DE-SC0018739.

REFERENCES

(1) Lussier, A. J.; Lopez, R. A. K.; Burns, P. C. A Revised and Expanded Structure Hierarchy of Natural and Synthetic Hexavalent Uranium Compounds. *Can. Mineral.* **2016**, *54* (1), 177−283.

(2) Alsobrook, A. N.; Hauser, B. G.; Hupp, J. T.; Alekseev, E. V.; Depmeier, W.; Albrecht-Schmitt, T. E. From Layered Structures to Cubic Frameworks: Expanding the Structural Diversity of Uranyl Carboxyphosphonates via the Incorporation of Cobalt. *Cryst. Growth Des.* **2011**, *11* (4), 1385−1393.

(3) Xiao, B.; Schlenz, H.; Dellen, J.; Bosbach, D.; Suleimanov, E. V.; Alekseev, E. V. From Two-Dimensional Layers to Three-Dimensional Frameworks: Expanding the Structural Diversity of Uranyl Compounds by Cation−Cation Interactions. *Cryst. Growth Des.* **2015**, *15* (8), 3775−3784.

(4) Yu, N.; Klepov, V. V.; Villa, E. M.; Bosbach, D.; Suleimanov, E. V.; Depmeier, W.; Albrecht-Schmitt, T. E.; Alekseev, E. V. Topologically Identical, but Geometrically Isomeric Layers in Hydrous α-, β-$Rb[UO_2(AsO_3OH)(AsO_2(OH)_2)]\cdot H2O$ and Anhydrous $Rb[UO_2(AsO_3OH)(AsO_2(OH)_2)]$. *J. Solid State Chem.* **2014**, *215* (0), 152−159.

(5) Wang, Z.; Zachara, J. M.; Gassman, P. L.; Liu, C.; Qafoku, O.; Yantasee, W.; Catalano, J. G. Fluorescence Spectroscopy of U(VI)-Silicates and U(VI)-Contaminated Hanford Sediment. *Geochim. Cosmochim. Acta* **2005**, *69* (6), 1391−1403.

(6) Xie, J.; Wang, Y.; Liu, W.; Yin, X.; Chen, L.; Zou, Y.; Diwu, J.; Chai, Z.; Albrecht-Schmitt, T. E.; Liu, G.; et al. Highly Sensitive Detection of Ionizing Radiations by a Photoluminescent Uranyl Organic Framework. *Angew. Chem., Int. Ed.* **2017**, *56* (26), 7500−7504.

(7) zur Loye, H.-C.; Besmann, T. M.; Amoroso, J.; Brinkman, K. S.; Grandjean, A.; Henager, C. H., Jr.; Hu, S.; Misture, S. T.; Phillpot, S. R.; Shustova, N. B.; Wang, H.; Koch, R. J.; Morrison, G.; Dolgopolova, E. A. Novel Approaches to Hierarchical Materials as Tailored Nuclear Waste Forms: A Perspective. *Chem. Mater.* **2018**, *30*, 4475−4488.

(8) Feng, M.-L.; Sarma, D.; Qi, X.-H.; Du, K.-Z.; Huang, X.-Y.; Kanatzidis, M. G. Efficient Removal and Recovery of Uranium by a Layered Organic−Inorganic Hybrid Thiostannate. *J. Am. Chem. Soc.* **2016**, *138* (38), 12578−12585.

(9) Morrison, G.; Smith, M. D.; zur Loye, H.-C. Understanding the Formation of Salt-Inclusion Phases: An Enhanced Flux Growth Method for the Targeted Synthesis of Salt-Inclusion Cesium Halide Uranyl Silicates. *J. Am. Chem. Soc.* **2016**, *138* (22), 7121−7129.

(10) Mesbah, A.; Prakash, J.; Ibers, J. A. Overview of the Crystal Chemistry of the Actinide Chalcogenides: Incorporation of the Alkaline-Earth Elements. *Dalton Trans* **2016**, *45* (41), 16067−16080.

(11) Malliakas, C. D.; Yao, J.; Wells, D. M.; Jin, G. B.; Skanthakumar, S.; Choi, E. S.; Balasubramanian, M.; Soderholm, L.;

DOI: 10.1021/acs.inorgchem.8b01733
Inorg. Chem. XXXX, XXX, XXX−XXX

Ellis, D. E.; Kanatzidis, M. G.; et al. Oxidation State of Uranium in $A_6Cu_{12}U_2S_{15}$ (A = K, Rb, Cs) Compounds. *Inorg. Chem.* **2012**, *51* (11), 6153−6163.
(12) Neuhausen, C.; Hatscher, S. T.; Panthöfer, M.; Urland, W.; Tremel, W. Comprehensive Uranium Thiophosphate Chemistry: Framework Compounds Based on Pseudotetrahedrally Coordinated Central Metal Atoms: Comprehensive Uranium Thiophosphate Chemistry. *Z. Anorg. Allg. Chem.* **2013**, *639* (15), 2836−2845.
(13) Gieck, C.; Tremel, W. Interlocking Inorganic Screw Helices: Synthesis, Structure, and Magnetism of the Novel Framework Uranium Orthothiophoshates $A_{11}U_7(PS_4)_{13}$ (A = K, Rb). *Chem. - Eur. J.* **2002**, *8* (13), 2980.
(14) Gieck, C.; Rocker, F.; Ksenofontov, V.; Gütlich, P.; Tremel, W. Supramolecular" Solid-State Chemistry: Interpenetrating Diamond-Type Frameworks of U^{4+} Ions Linked BγS,S′-Bidentate $P_2S_6^{2-}$ Molecular Rods in UP_4S_{12}. *Angew. Chem., Int. Ed.* **2001**, *40* (5), 908−911.
(15) Yeon, J.; Smith, M. D.; Tapp, J.; Möller, A.; zur Loye, H.-C. Application of a Mild Hydrothermal Approach Containing an in Situ Reduction Step to the Growth of Single Crystals of the Quaternary U(IV)-Containing Fluorides $Na_4MU_6F_{30}$ (M = Mn^{2+}, Co^{2+}, Ni^{2+}, Cu^{2+}, and Zn^{2+}) Crystal Growth, Structures, and Magnetic Properties. *J. Am. Chem. Soc.* **2014**, *136* (10), 3955−3963.
(16) Felder, J.; Yeon, J.; Smith, M.; zur Loye, H.-C. Application of a Mild Hydrothermal Method to the Synthesis of Mixed Transition-Metal(II)/Uranium(IV) Fluorides. *Inorg. Chem. Front.* **2017**, *4* (2), 368−377.
(17) Hess, R. F.; Abney, K. D.; Burris, J. L.; Hochheimer, H. D.; Dorhout, P. K. Synthesis and Characterization of Six New Quaternary Actinide Thiophosphate Compounds: $Cs_8U_5(P_3S_{10})_2(PS_4)_6$, $K_{10}Th_3(P_2S_7)_4$ $(PS_4)_2$, and $A_5An(PS_4)_3$, (A = K, Rb, Cs; An = U, Th). *Inorg. Chem.* **2001**, *40* (12), 2851−2859.
(18) Alekseev, E. V.; Krivovichev, S. V.; Malcherek, T.; Depmeier, W. Crystal Chemistry of Anhydrous Li Uranyl Phosphates and Arsenates. I. Polymorphism and Structure Topology: Synthesis and Crystal Structures of α-$Li[(UO_2)(PO_4)]$, α-$Li[(UO_2)(AsO_4)]$, β-$Li[(UO_2)(AsO_4)]$ and $Li_2[(UO_2)_3(P_2O_7)_2]$. *J. Solid State Chem.* **2008**, *181* (11), 3010−3015.
(19) Alekseev, E. V.; Krivovichev, S. V.; Depmeier, W.; Knorr, K. Complex Topology of Uranyl Polyphosphate Frameworks: Crystal Structures of α-, β-$K[(UO_2)(P_3O_9)]$ and $K[(UO_2)_2(P_3O_{10})]$. *Z. Anorg. Allg. Chem.* **2008**, *634* (9), 1527−1532.
(20) Bugaris, D. E.; Ibers, J. A. Syntheses and Characterization of Some Solid-State Actinide (Th, U, Np) Compounds. *Dalton Trans.* **2010**, *39* (26), 5949.
(21) Bugaris, D. E.; zur Loye, H.-C. Materials Discovery by Flux Crystal Growth: Quaternary and Higher Order Oxides. *Angew. Chem., Int. Ed.* **2012**, *51* (16), 3780−3811.
(22) *SAINT*; Bruker AXS Inc.: Madison, WI, 2012.
(23) Krause, L.; Herbst-Irmer, R.; Sheldrick, G. M.; Stalke, D. Comparison of Silver and Molybdenum Microfocus X-Ray Sources for Single-Crystal Structure Determination. *J. Appl. Crystallogr.* **2015**, *48* (1), 3−10.
(24) Dolomanov, O. V.; Bourhis, L. J.; Gildea, R. J.; Howard, J. A. K.; Puschmann, H. OLEX2: A Complete Structure Solution, Refinement and Analysis Program. *J. Appl. Crystallogr.* **2009**, *42* (2), 339−341.
(25) Sheldrick, G. M. Crystal Structure Refinement with *SHELXL*. *Acta Crystallogr., Sect. C: Struct. Chem.* **2015**, *71* (1), 3−8.
(26) Spek, A. Structure Validation in Chemical Crystallography. *Acta Crystallogr., Sect. D: Biol. Crystallogr.* **2009**, *65* (2), 148−155.
(27) Morrison, G.; zur Loye, H.-C. Simple Correction for the Sample Shape and Radial Offset Effects on SQUID Magnetometers: Magnetic Measurements on Ln_2O_3 (Ln = Gd, Dy, Er) Standards. *J. Solid State Chem.* **2015**, *221*, 334−337.
(28) Blatov, V. A.; Shevchenko, A. P.; Serezhkin, V. N. *TOPOS* 3.2: A New Version of the Program Package for Multipurpose Crystal-Chemical Analysis. *J. Appl. Crystallogr.* **2000**, *33* (4), 1193−1193.
(29) Blatov, V. A. Multipurpose Crystallochemical Analysis with the Program Package TOPOS. *IUCr CompComm Newslett.* **2006**, *7*, 4.
(30) Blatov, V. A.; Serezhkin, V. N. Stereoatomic Model of the Structure of Inorganic and Coordination Compounds. *Russ. J. Inorg. Chem.* **2000**, *45*, S105−S222.
(31) Blatov, V. A.; Shevchenko, A. P.; Proserpio, D. M. Applied Topological Analysis of Crystal Structures with the Program Package ToposPro. *Cryst. Growth Des.* **2014**, *14* (7), 3576−3586.
(32) Johnson, D.; Hils, J. Phosphate Esters, Thiophosphate Esters and Metal Thiophosphates as Lubricant Additives. *Lubricants* **2013**, *1* (4), 132−148.
(33) Behrle, A. C.; Kerridge, A.; Walensky, J. R. Dithio- and Diselenophosphinate Thorium(IV) and Uranium(IV) Complexes: Molecular and Electronic Structures, Spectroscopy, and Trans-metalation Reactivity. *Inorg. Chem.* **2015**, *54* (24), 11625−11636.
(34) Kepert, D. L. *Inorganic Stereochemistry*; Springer: Berlin, 1982.
(35) Serezhkin, V. N.; Vologzhanina, A. V.; Serezhkina, L. B.; Smirnova, E. S.; Grachova, E. V.; Ostrova, P. V.; Antipin, M. Y. Crystallochemical Formula as a Tool for Describing Metal−Ligand Complexes − a Pyridine-2,6-Dicarboxylate Example. *Acta Crystallogr., Sect. B: Struct. Sci.* **2009**, *65* (1), 45−53.
(36) Mesbah, A.; Prakash, J.; Beard, J. C.; Lebègue, S.; Malliakas, C. D.; Ibers, J. A. Syntheses, Crystal Structures, Optical and Theoretical Studies of the Actinide Thiophosphates $SrU(PS_4)_2$, $BaU(PS_4)_2$, and $SrTh(PS_4)_2$. *Inorg. Chem.* **2015**, *54* (6), 2970−2975.
(37) Neuhausen, C.; Rocker, F.; Tremel, W. Modular Metal Chalcogenide Chemistry: Secondary Building Blocks as a Basis of the Silicate-Type Framework Structure of $CsLiU(PS_4)_2$. *Z. Anorg. Allg. Chem.* **2012**, *638* (2), 405−410.
(38) O'Keeffe, M.; Peskov, M. A.; Ramsden, S. J.; Yaghi, O. M. The Reticular Chemistry Structure Resource (RCSR) Database of, and Symbols for, Crystal Nets. *Acc. Chem. Res.* **2008**, *41* (12), 1782−1789.
(39) Alexandrov, E. V.; Blatov, V. A.; Kochetkov, A. V.; Proserpio, D. M. Underlying Nets in Three-Periodic Coordination Polymers: Topology, Taxonomy and Prediction from a Computer-Aided Analysis of the Cambridge Structural Database. *CrystEngComm* **2011**, *13* (12), 3947.
(40) Chen, L.; Diwu, J.; Gui, D.; Wang, Y.; Weng, Z.; Chai, Z.; Albrecht-Schmitt, T. E.; Wang, S. Systematic Investigation of the *in Situ* Reduction Process from U(VI) to U(IV) in a Phosphonate System under Mild Solvothermal Conditions. *Inorg. Chem.* **2017**, *56* (12), 6952−6964.
(41) Yeon, J.; Smith, M. D.; Sefat, A. S.; Tran, T. T.; Halasyamani, P. S.; zur Loye, H.-C. U3F12(H2O), a Noncentrosymmetric Uranium-(IV) Fluoride Prepared via a Convenient In Situ Route That Creates U4+ under Mild Hydrothermal Conditions. *Inorg. Chem.* **2013**, *52* (15), 8303−8305.
(42) Carnall, W. T.; Liu, G. K.; Williams, C. W.; Reid, M. F. Analysis of the Crystal-field Spectra of the Actinide Tetrafluorides. I. UF_4, NpF_4, and PuF_4. *J. Chem. Phys.* **1991**, *95* (10), 7194−7203.

DOI: 10.1021/acs.inorgchem.8b01733
Inorg. Chem. XXXX, XXX, XXX−XXX